Divalent Metal Vinylphosphonate Layered Materials: Compositional Variability, Structural Peculiarities, Dehydration Behavior, and Photoluminescent Properties

Rosario M. P. Colodrero,[†] Aurelio Cabeza,[†] Pascual Olivera-Pastor,[†] Duane Choquesillo-Lazarte,[⊥] Juan M. Garcia-Ruiz,[⊥] Adele Turner,[∥] Gheorghe Ilia,[§] Bianca Maranescu,[§] Konstantinos E. Papathanasiou,[‡] Gary B. Hix,*[∥] Konstantinos D. Demadis,*[‡] and Miguel A. G. Aranda*[†]

[†]Departamento de Química Inorgánica, Universidad de Málaga, Campus Teatinos S/N. 29071-Málaga, Spain

[‡]Crystal Engineering, Growth and Design Laboratory, Department of Chemistry, University of Crete, Voutes Campus, Crete, GR-71003, Greece

[§]Institute of Chemistry Timisoara of Romanian Academy, Bd. Mihai Viteazul 24, R-300223 Timisoara, Romania

[⊥]Laboratorio de Estudios Crystalográficos, IACT-CSIC, Granada, Spain

[∥]School of Science and Technology, Nottingham Trent University, Clifton Lane, Nottingham, NG11 8NS, United Kingdom

S *Supporting Information*

ABSTRACT: A family of **M-VP** (M = Ni, Co, Cd, Mn, Zn, Fe, Cu, Pb; VP = vinylphosphonate) and **M-PVP** (M = Co, Cd; PVP = phenylvinylphosphonate) materials have been synthesized by hydrothermal methods and characterized by FT-IR, elemental analysis, and thermogravimetric analysis (TGA). Their structures were determined either by single crystal X-ray crystallography or from laboratory X-ray powder diffraction data. The crystal structure of some **M-VP** and **M-PVP** materials is two-dimensional (2D) layered, with the organic groups (vinyl or phenylvinyl) protruding into the interlamellar space. However, the **Pb-VP** and **Cu-VP** materials show dramatically different structural features. The porous, three-dimensional (3D) structure of **Pb-VP** contains the Pb center in a pentagonal pyramid. A **Cu-VP** variant of the common 2D layered structure shows a very peculiar structure. The structure of the material is 2D with the layers based upon three crystallographically distinct Cu atoms; an octahedrally coordinated Cu^{2+} atom, a square planar Cu^{2+} atom and a Cu^+ atom. The latter has an unusual co-ordination environment as it is 3-coordinated to two oxygen atoms with the third bond across the double bond of the vinyl group. Metal-coordinated water loss was studied by TGA and thermodiffractometry. The rehydration of the anhydrous phases to give the initial phase takes place rapidly for **Cd-PVP** but it takes several days for **Co-PVP**. The **M-VP** materials exhibit variable dehydration—rehydration behavior, with most of them losing crystallinity during the process.
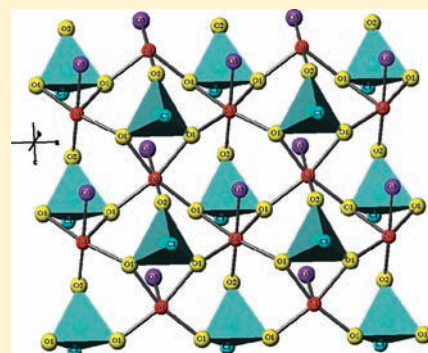
■ INTRODUCTION

Metal phosphonate materials, $M(O_3PR)_x \cdot yH_2O$, represent a class of inorganic—organic hybrid materials which are receiving increasing attention in the literature. Unlike metal organic framework materials (MOFs) these materials are generally based around a relatively robust inorganic metal phosphate framework but may contain organic functional groups which in the majority of cases play no part in maintaining the crystal structure. With this in mind, many researchers see metal phosphonates as potential functional materials in a variety of applications, with the particular application being dependent upon the organic functional groups present. Materials containing carboxylic[1−10] or sulfonic acid groups[11−15] have potential application as acid—base catalysts,[16−18] ion exchange materials,[19,20] or proton conducting materials;[21,22] those containing amines[23−27] might find use as sorbents or metal sequestering agents.

Other potential applications rely upon the electronic structure of the organic group. For example, conjugated π-bonded systems are well-known for their ability to absorb UV light, with the extent of conjugation determining the wavelength of the absorption maximum. In this sense they can act almost as an antenna for the absorption of light energy. This energy can then excite electronic transitions in neighboring metal atoms, giving rise to the observation of luminescent properties. Indeed there have been a number of phenylphosphonate and related materials which contain lanthanoids reported in the literature which exhibit such properties.[28] Materials of this type may lend themselves to applications in the generation of solar power.

In metal phosphonates where the organic functional group is not bonded directly to the metal there also exists the possibility to modify the organic group by carrying out reactions within the metal phosphonate. For example, it is a relatively simple matter

ACS Publications © 2011 American Chemical Society

11202

dx.doi.org/10.1021/ic201760w | *Inorg. Chem.* 2011, 50, 11202–11211

Table 1. Layered Metal Unsaturated Phosphonates in This Study[a]

material	synthesis pH	T (°C)	chemical formula	metal coordination	reference
Ni-VP	2.8−3.1	65−80	$Ni(O_3PCH{=}CH_2)\cdot H_2O$	distorted octahedral	this work
Co-VP	2.8−3.1	65−80	$Co(O_3PCH{=}CH_2)\cdot H_2O$	distorted octahedral	this work
Cd-VP	2.8−3.1	65−80	$Cd(O_3PCH{=}CH_2)\cdot H_2O$	distorted octahedral	this work
Mn-VP	2.8−3.1	65−80	$Mn(O_3PCH{=}CH_2)\cdot H_2O$	distorted octahedral	this work
Zn-VP	4.3−4.5	160	$Zn(O_3PCH{=}CH_2)\cdot H_2O$	distorted octahedral	Shannon[39]
Fe-VP	4.3−4.5	160	$Fe(O_3PCH{=}CH_2)\cdot H_2O$	distorted octahedral	this work
Cu-VP(1)	4.3−4.5	160	$Cu(O_3PCH{=}CH_2)\cdot H_2O$	square pyramidal	Shannon,[39] Knight[40]
Cu-VP(2)	4.3−4.5	160	$Cu_2(O_3PCH{=}CH_2)(OH)$	distorted octahedral (Cu^{2+}), square planar (Cu^{2+}), 3-coordinate (Cu^+)	this work
Pb-VP	4.3−4.5	160	$Pb(O_3PCH{=}CH_2)\cdot H_2O$	pentagonal pyramidal	Hix[42]
Co-PVP	2.8−3.1	65−80	$Co(O_3PC(Ph){=}CH_2)\cdot H_2O$	distorted octahedral	this work
Cd-PVP	2.8−3.1	65−80	$Cd(O_3PC(Ph){=}CH_2)\cdot H_2O$	monocapped octahedron	this work

[a] VP = vinylphosphonate; PVP = phenylvinylphosphonate.

to carry out a substitution reaction on the phenyl ring within zirconium phenyl phosphonate.[29] This means that it is no longer necessary to directly synthesize a phosphonic acid precursor for the synthesis of a material with a particular function; this might prove important if the desired group is one which is likely to become attached to metal ions in the synthesis of the hybrid material. For this purpose suitable organic synthons are required. The vinyl moiety represents one such group, which is also attractive from the point of view of luminescent materials as it will undergo a $\pi-\pi^*$ transition upon absorbing light of the appropriate wavelength.

In this paper we describe the synthesis and the structural and physicochemical characterization of a number of metal vinylphosphonates, $M(O_3PCH{=}CH_2)_x \cdot yH_2O$, and phenylvinylphosphonates, $M(O_3PC(Ph){=}CH_2)_x \cdot yH_2O$. In one of these materials we also describe an unprecedented structural motif in the crystal chemistry of metal vinylphosphonates, where the metal (copper) is present in two different oxidation states and the vinyl group is actively participating in maintaining the structure. Furthermore, taking advantage the response of the vinyl group to UV light, we describe herein the luminescent properties of a number of these materials and compare them to related metal phenylphosphonates.

■ EXPERIMENTAL SECTION

The materials synthesized in this paper are presented in Table 1, together with their abbreviations used throughout the paper, details regarding their synthesis conditions and metal coordination motif.

Materials. All reagents were used as received from the supplier (Aldrich) without further purification. In-house, deionized (DI) water was used for all syntheses. Water-soluble metal salts were commercial samples and were used without further purification.

Instrumentation. Elemental analyses (CHN) were measured on a Perkin−Elmer 240 or a Carlos Elba 1011 analyzer. Thermogravimetric analysis (TGA) data were recorded on a Perkin-Elmer Diamond device under air flow. The temperature was varied from room temperature (RT) to 1000 °C at a heating rate of 10 °C·min^{-1}. Measurements were carried out on samples in open platinum crucibles under air flow. Infrared spectra were obtained with an ATR accessory (MIRacle ATR, PIKE Technologies, U.S.A.) coupled to FTIR spectrometer (FT/IR-4100, JASCO, Spain), or a Nicolet 5DXC spectrometer. All spectra were recorded in the 4000 to 600 cm^{-1} range at 4 cm^{-1} resolution and 50 scans were accumulated.

Diffuse reflectance UV−vis spectra were recorded using a Jasco V-670 spectrophotometer with a 60 mm integrating sphere. Photoluminescence spectra were recorded using the fourth harmonic of a Nd:Yag laser which excites the samples with radiation of $\lambda = 266$ nm. For the standard PL spectra setup, an optical fiber is utilized to transmit the fluorescence signal to a UV−visible (300−1000 nm) spectrometer (S2000, Ocean Optics Inc. (OOI)) and the acquired spectrum can be interpreted via OOI software. A background spectrum of an empty sample holder was recorded prior to the sample spectra, which showed no response to the laser excitation. The materials were also investigated to see if there was any emission in the IR region (1000−2000 nm), but no responses were observed.

Syntheses of **M-PVP** *(M = Cd, Co; PVP = Phenylvinylphosphonate)* *and* **M-VP** *(M = Cd, Co, Ni; VP = Vinylphosphonate) Materials.* A 100 mL round-bottomed flask was charged with M^{2+} salt (sulfate or nitrate, 50.0 mmol), phenylvinylphosphonic (50.0 mmol) or vinylphosphonic acid (50.0 mmol), urea (50.0 mmol), and distilled water (50 mL). The pH was adjusted to 2.8−3.1 with an aqueous solution of NaOH (0.10 M). The solution was heated in an oil-bath at 65−80 °C for 75−80 h. The resulting crystals were collected by filtration, washed with distilled water and dried in air (yield: 60−78%).

Synthesis of **M-VP** *(M = Mn, Zn, Fe, Cu, Pb) Materials.* All materials were formed by a hydrothermal reaction between the relevant metal acetate(s) and either vinylphosphonic acid or diethyl vinylphosphonate. In all cases except that of Cu (**Cu-VP(2)**, see below) the products are the same, with the only notable difference being the crystallinity of the products. Typical syntheses followed a standard method in which equimolar quantities of metal acetate and the diethyl vinylphosphonate ester (or vinylphosphonic acid) (3.7 mmol) are used. The metal acetate is mixed with 10 mL of distilled water and stirred until it has dissolved before the phosphonate ester or phosphonic acid is added. The mixture is then placed in a Teflon lined stainless steel autoclave with a capacity of 23 mL. The autoclave was then heated under autogenous pressure at 160 °C for two days. After this time the product was recovered by filtration, washed in distilled water, and allowed to dry in air. It was observed that samples prepared using phosphonate esters tended to have larger crystals than those prepared from the corresponding phosphonic acid.

Synthesis of $Cu_2(O_3PCH{=}CH_2)(OH)$, **Cu-VP(2)**. This material was synthesized by reaction between copper acetate, $Cu(CH_3CO_2)_2 \cdot H_2O$, and diethyl vinylphosphonate; the reaction between Cu acetate and vinylphosphonic acid results in the formation of **Cu-VP(1)**. In a typical experiment 3.7 mmol of metal acetate are dissolved in 10 mL of distilled water. The solution is stirred until the acetate has dissolved, after which 3.7 mmol of diethyl vinylphosphonate are added. The reaction mixture is stirred for an additional 15 min, then transferred to a Teflon lined autoclave which has a fill capacity of 23 mL. The autoclave is placed in an oven at 160 °C for 2 days, after which it is removed and allowed to cool.

Table 2. Crystallographic Data for M-VP and M-PVP Materials

	phase				
	Co-VP	**Ni-VP**	**Cd-VP**	**Co-PVP**	**Cd-PVP**
empirical formula	$C_2H_5CoO_4P$	$C_2H_5NiO_4P$	$C_2H_5CdO_4P$	$C_8H_9CoO_4P$	$C_8H_9CdO_4P$
F.W. $(g \cdot mol^{-1})$	182.93	182.69	236.40	259.05	312.47
space group	$Pmn21$	$Pmn21$	$Pmn21$	Pn	Pn
λ (Å)	1.5406	1.5406	1.5406	1.54178	1.5406
a (Å)	5.66454(23)	5.59305(11)	5.92775(25)	4.9388(11)	5.18330(21)
b (Å)	9.82816(32)	9.80728(19)	9.94341(30)	15.844(4)	15.3959(5)
c (Å)	4.79868(21)	4.74367(13)	5.03132(27)	5.7119(13)	5.94949(21)
α (deg)	90.0	90.0	90.0	90.0	90.0
β (deg)	90.0	90.0	90.0	92.201(12)	94.5304(33)
γ (deg)	90.0	90.0	90.0	90.0	90.0
V (Å^3)	267.152(22)	260.203(14)	296.556(21)	446.63(18)	473.29(4)
crystal size (mm)				$0.07 \times 0.04 \times 0.02$	
Z	2	2	2	2	2
V (Å^3 atom^{-1})^a	16.697	16.263	18.535	15.951	16.903
ρ_{calc} $(g \cdot cm^{-3})$	2.212	2.268	2.591	1.926	2.129
2θ range (deg)	16−76.5	16−109.8	19−90	2.79−66.03	10−109.98
data/restrains/parameters	3572/10/33	5530/10/47	4185/10/53	5602/2/164	3862/38/78
no. reflections	95	205	155	1412	292
R_{wp}	0.0101	0.0654	0.0494	-	0.0703
R_p	0.0070	0.0483	0.0361	-	0.0528
R_F	0.0536	0.0614	0.0306	-	0.0425
GoF, F^2				1.008	
R Factor $[I > 2\sigma(I)]$				^{b}R1 = 0.0767	
				^{b}wR2 = 0.0723	
R Factor (all data)				^{b}R1 = 0.1887	
				^{b}wR2 = 0.1822	
CCDC reference code	688270	688271	688269	688268	809977

	phase			
	Cu-VP2	**Fe-VP**	**Zn-VP**	**Pb-VP**
empirical formula	$C_2H_4Cu_2O_4P$	$C_2H_5FeO_4P$	$C_2H_5FeO_4P$	$C_2H_3O_3PbP$
F.W. $(g \cdot mol^{-1})$	250.1	177.86	189.4	313.20
space group	$P2_1/n$	$Pmn2_1$	$Pmn2_1$	$R\bar{3}$
λ (Å)	1.54178	0.71073	0.71073	1.54178
a (Å)	5.3436(3)	5.66454(9)	5.6700(4)	19.9834(4)
b (Å)	16.8317(7)	9.82816(2)	9.7080(7)	19.9834(4)
c (Å)	6.0766(3)	4.79868(9)	4.7747(3)	6.8829(2)
α (deg)	90.0	90.0	90.0	90.0
β (deg)	109.478(3)	90.0	90.0	90.0
γ (deg)	90.0	90.0	90.0	120.0
V (Å^3)	515.26(4)	267.86(9)	262.82(3)	2380.35(10)
Z	4	2	2	18
V (Å^3 atom^{-1})^a	14.313	16.741	16.426	18.892
ρ_{calc} $(g \cdot cm^{-3})$	3.224	2.205	2.393	3.933
2θ range (deg)	5.26−70.40	4.14−27.38	4.16−32.3	4.42−70.36
data/restrains/parameters	923/0/102	662/2/47	986/2/46	966/0/64
no. reflections	2689	3399	8281	3594
independent reflections $[I > 2\sigma(I)]$	870	547	896	966
GoF, F^2	1.090	1.071	1.166	1.114
R Factor $[I > 2\sigma(I)]$	^{b}R1 = 0.0378	^{b}R1 = 0.0593	^{b}R1 = 0.0407	^{b}R1 = 0.0457
	^{b}wR2 = 0.1051	^{b}wR2 = 0.1286	^{b}wR2 = 0.0904	^{b}wR2 = 0.1143

Table 2. Continued

	phase			
	Cu-VP2	**Fe-VP**	**Zn-VP**	**Pb-VP**
R Factor (all data)	[b]R1 = 0.0394	[b]R1 = 0.0795	[b]R1 = 0.0513	[b]R1 = 0.0468
	[b]wR2 = 0.1065	[b]wR2 = 0.1409	[b]wR2 = 0.0960	[b]wR2 = 0.1155
CCDC reference code	839381	839382	839384	839383

[a] Volume per non-hydrogen atom. [b] $R1(F) = \Sigma ||F_o| - |F_c||/\Sigma|F_o|$; $wR2(F^2) = [\Sigma w(F_o^2 - F_c^2)^2/\Sigma F^4]^{1/2}$.

The product is recovered by filtration, washed with distilled water, and allowed to dry in air.

Structural Determinations. Single Crystal X-ray Crystallography. Suitable single crystals of **Co-PVP** were obtained from the synthesis experiment. Thus, a single crystal was mounted on a glass fiber and used for data collection. Data were recorded in a Bruker X8 Proteum diffractometer at 293 K using Cu radiation. The data were processed with APEX2[30] and corrected for absorption using SADABS.[31] The structure was solved by direct methods,[32] revealing the positions of all non-hydrogen atoms. These atoms were refined on F^2 by full matrix least-squares procedure[33] using anisotropic displacement parameters. All hydrogens, except those of water molecules placed geometrically, were located in difference Fourier maps and included as fixed contributions riding on attached atoms with isotropic thermal displacement parameters 1.2 times those of the respective atom. Crystallographic and structure refinement data are also given in Table 2.

Single crystal data measurements for compounds **M-VP** (M = Mn, Zn, Fe, Mg, Cu, Pb; VP = vinylphosphonate) were carried out using a Rigaku R-Axis II image plate diffractometer using a rotating anode generator with Mo Kα radiation (λ = 0.71069 Å). Data were collected at 23 °C. The crystals were mounted on a glass fiber using an epoxy resin. A total of 36 images covering 180° were recorded. Structure solution, carried out by direct methods, using the SHELXS program,[32] revealed the location of all non-hydrogen atoms, which were refined anisotropically using SHELXL.[33] The H atoms were typically either located in the Fourier difference map or placed geometrically. Subsequent refinement of the displacement parameters of the hydrogen atoms was carried out isotropically in all cases.

Structure Determinations by X-ray Powder Diffraction. Laboratory X-ray powder diffraction (XRPD) patterns were collected on a PANalytical X'Pert Pro diffractometer in a Bragg–Brentano reflection configuration by using a Ge(111) primary monochromator (Cu Kα_1) and the X'Celerator detector. XRPD patterns corresponding to **M-VP** (M = Ni, Co. and Cd) and **Cd-PVP** were autoindexed using the DICVOL06 program,[34] and the space groups were derived from the observed systematic extinctions. To minimize the preferred orientation effects, the powder patterns were collected in a sample disordered in the tubular aerosol suspension chamber (TASC) as previously reported.[35] Further details of the powder data collection and analysis are given in Table 2. The crystal structures of **Cd-PVP**, **Cd-VP**, and **Ni-VP** were solved *ab initio* using the automatic procedure in the program EXPO2004.[36] In those cases in which the initial structural models were unfinished, the missing atoms were localized by difference of Fourier maps. The **Co-VP** structure was obtained by Rietveld refinement from **Ni-VP**.

All crystal structures were refined by the Rietveld method[37] by using the GSAS package[38] with soft constraints to maintain chemically reasonable geometries for the phosphonate, vinyl, and phenyl groups. The soft constrains set were as follows: /PO$_3$C tetrahedron/P–O [1.53(1) Å], P–C [1.80(1) Å], O···O [2.55(1) Å], O···C [2.73(1) Å], /vinyl group/C═C [1.33(1) Å], P···C$_{vinyl}$ [2.72(2) Å], /phenyl group/C$_{vinyl}$-C$_{ring}$ [1.50(1) Å], C–C [1.40(1) Å], C$_{ring}$···C$_{ring}$ [2.38(2) Å] and C$_{ring}$···C$_{ring}$ [2.72(2) Å]. The final weight factors for the soft constrains histograms were of 10 for **M-VP** (M = Co, Ni, Cd) and 20 for **Cd-PVP**. No attempts to locate the H atoms were carried out

because of the limited quality of the powder diffraction data. Selected crystallographic and refinement details are given in Table 2. For **Ni-VP** one isotropic thermal displacement parameter was refined for Ni and P atoms and another for the rest of the atoms. For Co and Cd vinylphosphonate the isotropic thermal displacement parameters were fixed to 0.01 Å^2. Two isotropic thermal displacement parameters were refined for **Cd-PVP**, one for Cd and another one for the rest of the atoms. Crystallographic data are presented in Table 2, and the final Rietveld plots for compounds **Cd-PVP**, **Cd-VP**, **Co-VP**, and **Ni-VP** are given in the Supporting Information. Crystal structures have been deposited at the CCDC, and the reference codes are also given in Table 2.

The thermodiffractometric studies for **M-VP** and **M-PVP** were carried out for the sample loaded in an Anton Paar TTK450 Camera under static air. Flow of gases was not employed to avoid sample dehydration prior to the diffraction experiment. Data were collected at RT, 250 °C and RT after heating, a delay time of 10 min to ensure thermal stabilization. The data acquisition range was 4–50° (2θ) with a step size of 0.017°.

■ RESULTS

Structures of Metal-VP Materials. All metal vinylphosphonate and phenylvinylphosphonate materials, with the exception of **Pb-VP** are two-dimensional (2D) layered frameworks. The inorganic layer is composed of a metal–oxygen network. With the exception of **Cu-VP(2)**, which differs somewhat and will be described separately, the organic parts (vinyl or phenylvinyl) extend into the interlamellar space, held together by van der Waals forces. Here, we will briefly discuss the main structural features of this motif.

Compounds **M-VP** (M = Cd, Co, Ni, Zn, Fe) are isostructural. Two representative views of the structure are given in Figure 1.

The coordination geometry of the divalent metal center can best be described as a distorted octahedron. Four VP ligands coordinate the metal center via five phosphonate oxygens. Three VP ligands offer one oxygen each, whereas the fourth VP ligand acts as a bidentate chelate (4-membered ring). The sixth coordination site is occupied by a water molecule.

The vinyl groups are positioned in the interlamellar space in an interlocked fashion. The closest C···C contact between neighboring vinyl groups within the same layer is 5.670 Å. The closest C···C contact between vinyl groups from two adjacent layers is 3.866 Å. The positioning between vinyl groups of two neighboring layers is nearly perpendicular; hence there are no $\pi-\pi$ interactions. The closest M···M distance between metal centers from two adjacent layers is ~10.8 Å. While this paper was in preparation the crystal structure of **Cd-VP** was reported from single crystal data by the Knight group.[40b] Their structure is the same as ours, obtained from powder diffraction data.

Knight et al.[40] and Shannon et al.[39] have reported simultaneously on a Cu-vinylphosphonate 2D material which exhibits a 5-coordinated copper atom coordination sphere, and the
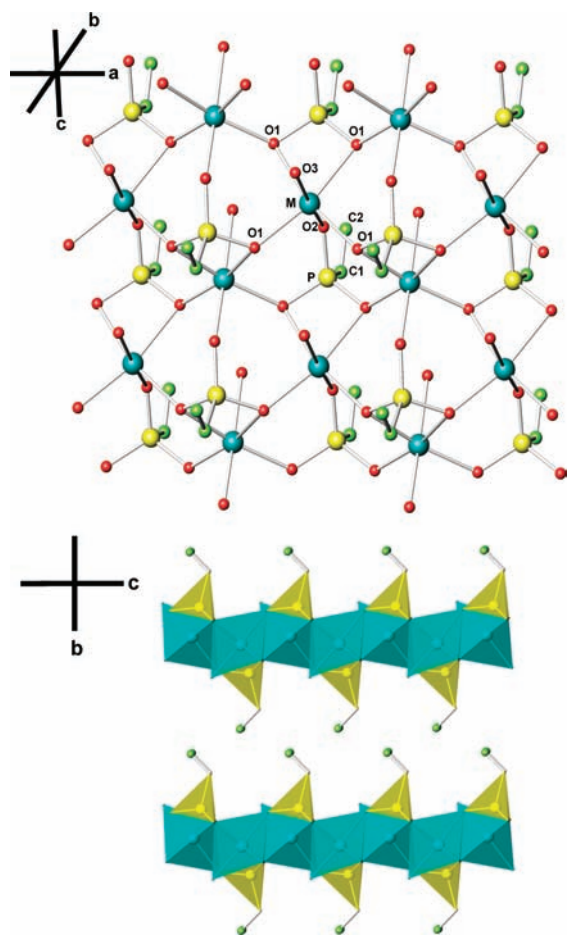
11205

dx.doi.org/10.1021/ic201760w |*Inorg. Chem.* 2011, 50, 11202–11211

Figure 1. Common layered structure of compounds **M-VP** (M = Cd, Co, Ni, Zn, Fe). Top: portion of one layer viewed from top. Bottom: two adjacent layers showing the vinyl groups pointing into the interlayer space.

geometry is best described as a distorted tetragonal pyramid similar to that observed for the copper methyl and phenylphosphonates, $[Cu(CH_3PO_3)]\cdot H_2O$, and $[Cu(C_6H_5PO_3)]\cdot H_2O$,[41] in which three phosphonate oxygens, and a coordinated water molecule make up the base of the pyramid.

Hix et al. solved the structure of Pb-vinylphosphonate.[42] The porous structure of lead vinylphosphonate is completely different to that of any previously reported divalent metal vinylphosphonate. The three-dimensional (3D) nature of the **Pb-VP** material is due to the much larger Pb^{2+}. The crystal structure contains one crystallographically distinct Pb atom, which is coordinated by six phosphonate oxygens. The coordination environment is best described as pentagonal pyramidal, with the lengths of the equatorial Pb—O bonds in the range 2.254—2.829 Å, whereas the axial Pb—O bond length is 2.254 Å. The five equatorial oxygen atoms form a distorted, nonplanar pentagon. The Pb atom is situated just below the pentagon. These polyhedra are joined to one another by corner sharing such that a spiral chain is formed in the [001] direction.

Structure of Cu-VP(2), $Cu_2(O_3PCH{=}CH_2)(OH)$. This material crystallizes in the $P2_1/n$ (No.14) space group, and the crystallographic data are presented in Table 2. The composition of $Cu_2(O_3PCH{=}CH_2)(OH)$ **Cu-VP(2)** derived from the single crystal data analysis is consistent with the CHN analysis results (see Supporting Information).

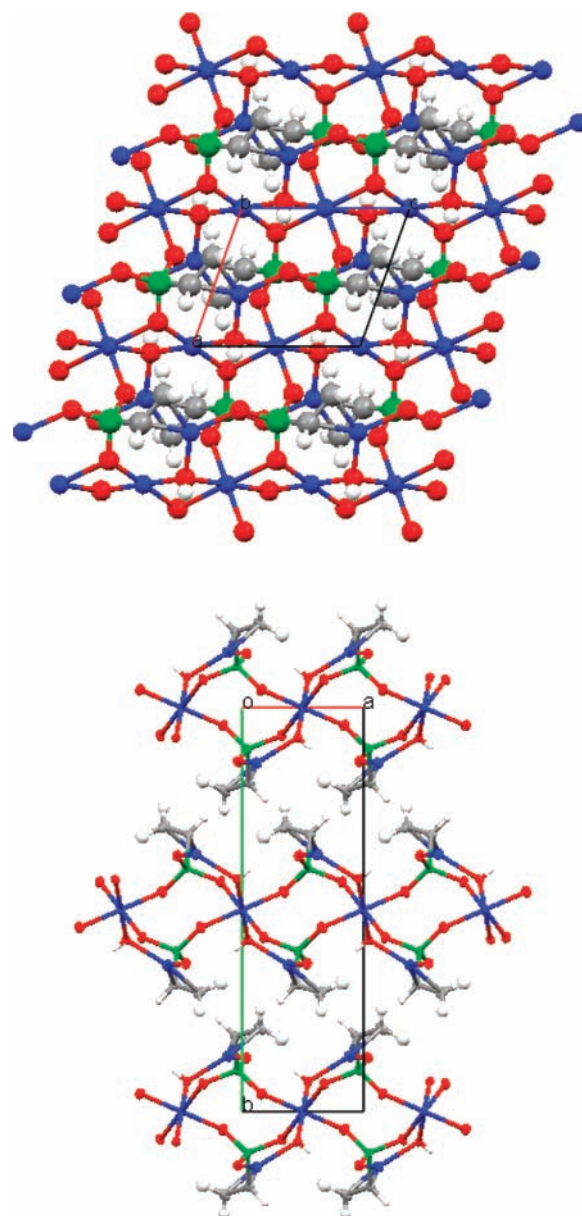**Figure 2.** Top: $Cu_2(O_3PCH{=}CH_2)(OH)$ viewed along the b axis showing the layered structure of the material. Bottom: $Cu_2(O_3PCH{=}CH_2)(OH)$ viewed along the c axis showing the co-ordination of the metal atoms. (Blue circles are Cu atoms, red circles are oxygen atoms, green circles are phosphorus atoms, black circles are carbon atoms, and white circles are hydrogen atoms).

The structure of the material is layered, with the vinyl groups projecting into the interlayer region as shown in Figure 2. While the distance between the copper atoms in neighboring layers is ~8.415 Å, these neighbors are offset from one another because of the crystallographic symmetry, and hence the length of the b axis is double the interlayer distance. The layers are based upon three crystallographically distinct Cu atoms; an octahedrally coordinated Cu^{2+} atom, a square planar Cu^{2+} atom, and a Cu^+ atom. The octahedrally coordinated Cu atom and square planar Cu atoms are linked by corner sharing oxygen atoms to form chains in the c direction, and are cross-linked by phosphate groups in the a direction to form layers in the ac plane. These layers then stack in the b direction (Figure 2).
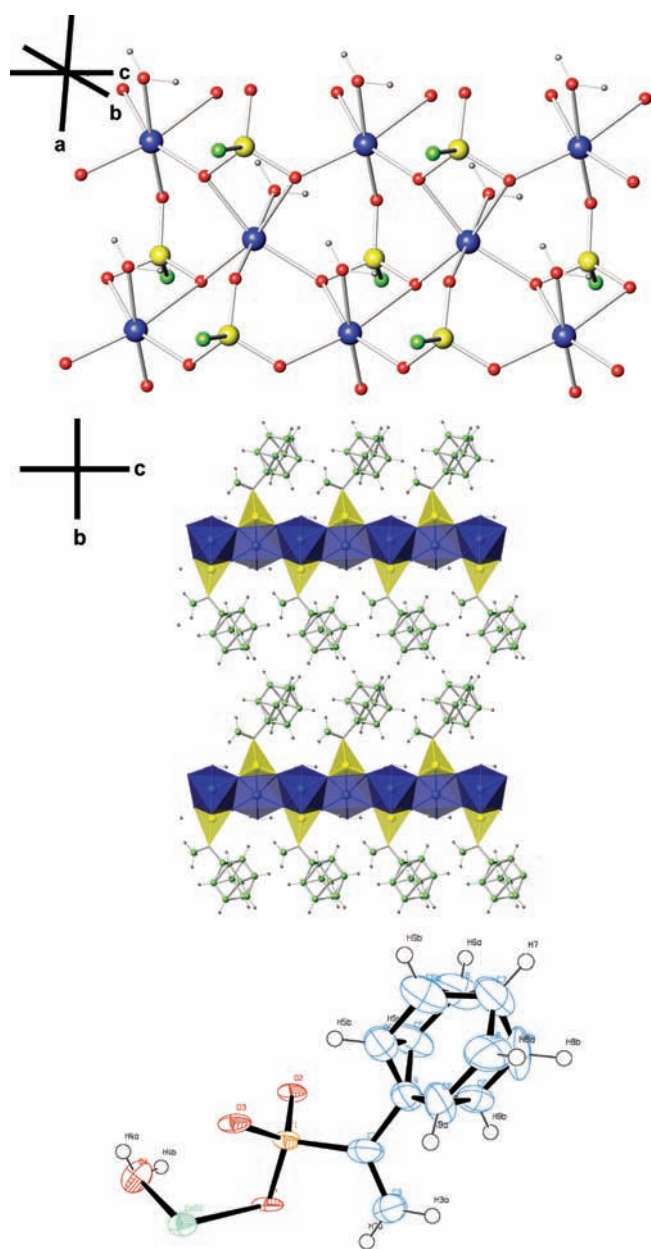
Figure 3. Crystal structure of $Co(O_3PC(Ph)=CH_2) \cdot H_2O$, **Co-PVP**. Top: portion of one layer viewed from the top. Middle: two adjacent layers showing the vinyl and phenyl groups, pointing into the interlayer space. Bottom: the disorder of the phenyl groups. Thermal ellipsoids shown at the 50% probability level.

The CuO_6 octahedron is elongated by a Jahn—Teller effect which is well-known for Cu^{2+}. This effect is reported by Barthelet et al. for MIL-55 and MIL-56,[43] by Drummel et al. for two copper hydroxyphosphonates,[44] and by Demadis et al.[45]

The Cu^+ site in the structure has an unusual co-ordination environment as it is 3 coordinate to two oxygen atoms with the third bond across the double bond of the vinyl group (Figure 2). The pseudotrigonal planar co-ordination of the Cu^+ ion is very similar to that reported for complexes containing such motifs reported elsewhere.[46] The Cu—C distances are 2.013 Å and 2.017 Å respectively. All five atoms (two carbon, two oxygen, and one copper) lie in the trigonal plane. The angles formed between the C=C centroid with the Cu and O atoms in the plane are 119.88° and 125.80°.
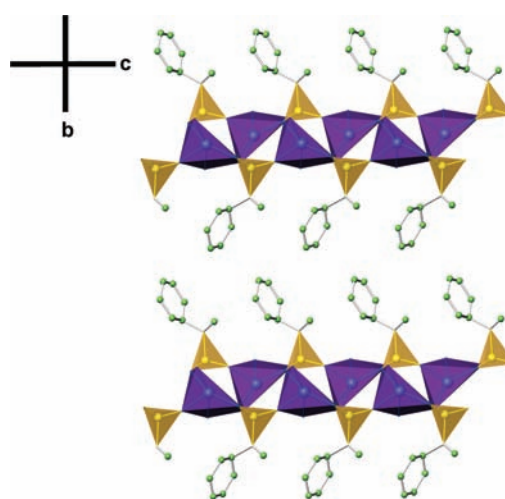

Figure 4. Crystal structure of $Cd(O_3PC(Ph)=CH_2) \cdot H_2O$, **Cd-PVP** showing two adjacent layers with the vinyl and phenyl groups, pointing into the interlayer space. The CdO_7 polyhedra are shown in purple.

The OH groups in this material bridge three Cu atoms. A similar feature is seen in some metal hydroxy phosphates such as $M^{II}_2(OH)(PO_4)$ where M = Zn and Co.[47] If the phosphate is replaced by a phosphonate group there should be a charge imbalance that would require the presence of an additional anion, as demonstrated for example by the NO_3^- ion in Cu^{II}_2-$(O_3P(CH_2)_2NH_2)(OH)(NO_3) \cdot H_2O$.[43] This is not the case in $Cu_2(O_3PCH=CH_2)(OH)$ because of the presence of both Cu^+ and Cu^{2+} ions.

Structures of Metal-PVP Materials. Of the two structurally characterized compounds (**Co-PVP** and **Cd-PVP**) **Co-PVP** shows the same structural motif as the **M-VP** (M = Cd, Co, Ni, Zn, Fe) compounds. Specifically, the Co coordination geometry is a slightly distorted octahedron. Because of the presence of the bulky phenyl rings, the interlayer distance is much higher, as evidenced by the closest Co···Co distance of 16.658 Å. Salient structural features of the structure of **Co-PVP** are presented in Figure 3. The phenyl groups were found to possess a rotational disorder (Figure 3, bottom). The positions of the disordered phenyl rings form a 65.14° angle.

The structure of $Cd(O_3PC(Ph)=CH_2) \cdot H_2O$, **Cd-PVP** (Figure 4) is a layered 2D architecture, but different from that of **Co-PVP**, principally because of the presence of the much larger Cd^{2+}, resulting in a higher coordination number of 7. The coordination geometry of Cd^{2+} could best be described as a monocapped octahedron. Two VP ligands act as bidentate chelates (forming 4-membered rings with the Cd). The remaining three coordination sites are occupied by two bridging phosphonate oxygens (originating from the chelating phosphonate groups) and one water molecule.

In Figure 5 we gathered all significant features regarding the metal centers (ligand identity, coordination geometry, bond lengths) for all available **M-VP** and **M-PVP** compounds.

Thermal Behavior of M-PVP and M-VP Materials. TGAs for **M-PVP** and **M-VP** compounds are displayed in Figure 6. In general, the TGA curves for **M-PVP** show a first well-defined step corresponding to the loss of the metal-coordinated water molecule between 110 and 170 °C, with an experimental associated weight loss of ~6.22% (calculated 5.77%) for **Cd-PVP** and 7.0% (calculated 6.95%) for **Co-PVP**. The thermal
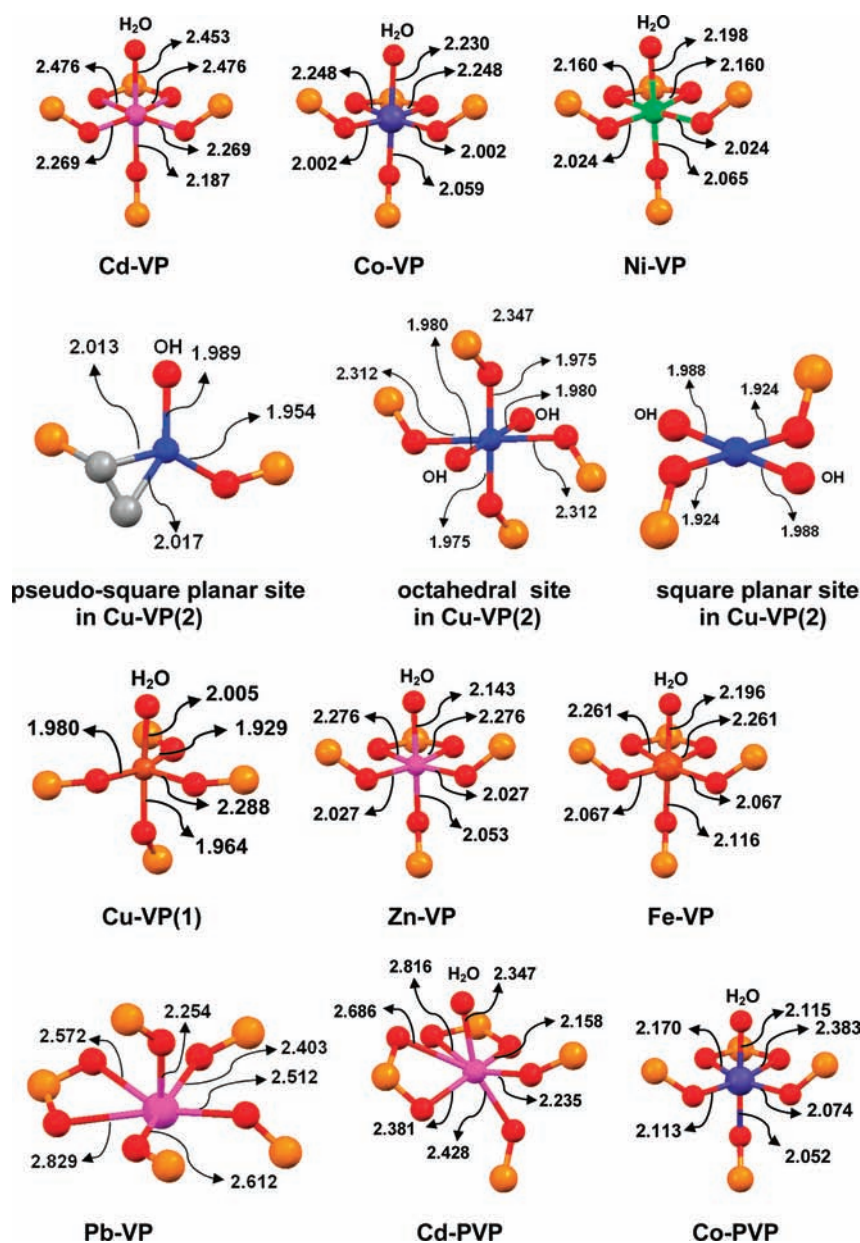
Figure 5. Coordination geometries of metal centers in **M-VP** and **M-PVP** materials.

stability of the resulting anhydrous phases depends upon the metal cation. Thus, while the organic component of **Cd-PVP** starts to decompose over 290 °C, **Co-PVP** is stable up to 390 °C.

The dehydration process (see Supporting Information) causes loss of crystallinity as well as a slight increase in the interlamellar space for both compounds. The position of the first peak shifts from 15.61 Å to 16.16 Å for **Cd-PVP** and from 15.87 Å to 16.38 Å for **Co-PVP**, Figure 7. This behavior could be due to a reordering of the phenyl groups into the interlamellar space after the elimination of the water molecule coordinated to the metal. The rehydration of the anhydrous phases to give the initial phase takes place rapidly for **Cd-PVP** but it takes several days for **Co-PVP**.

The TGA of **M-VP** (M = Co, Ni and Cd) compounds shows similar TGA curves with two main weight losses. The first one corresponds to the loss of the metal-coordinated water molecule. This process takes place at lower temperature, between 100 and

150 °C, for **Co-VP** with an associated weight loss of 11.00%, closely corresponding to the theoretical 9.85%. The semicrystal-line anhydrous phase shows a lower interlamellar space compared to the monohydrated compound and stays stable until 500 °C. The rehydration of this phase exposed to the air takes place after several hours, although the initial crystallinity is not recovered. This is shown in Figure 8.

Ni-VP exhibits higher thermal stability. This compound loses the water molecule between 208 and 264 °C, with a mass loss of 13.00% (calculated 9.80%). This difference may be due to a small amount of physisorbed water on the sample. The thermal behavior of **Cd-VP** is characterized by a gradual weight loss between 50 and 150 °C (observed 7.29% and calculated 7.62% for a water molecule), that overlaps with the combustion of the organic moieties.

Electronic (UV−vis) and Photoluminescence (PL) Spectra. The absorption spectra of all vinylphosphonates (Figure 9)
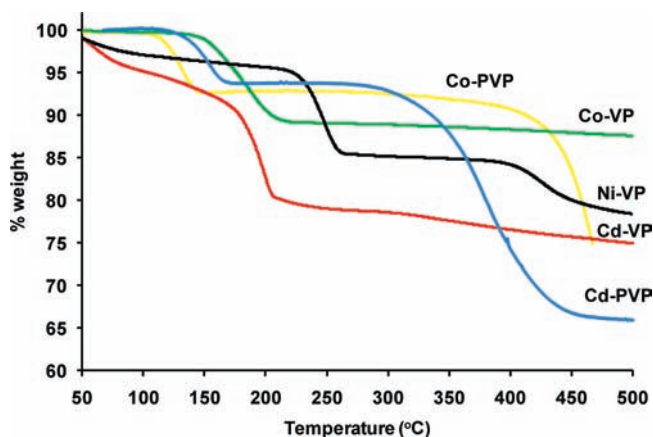
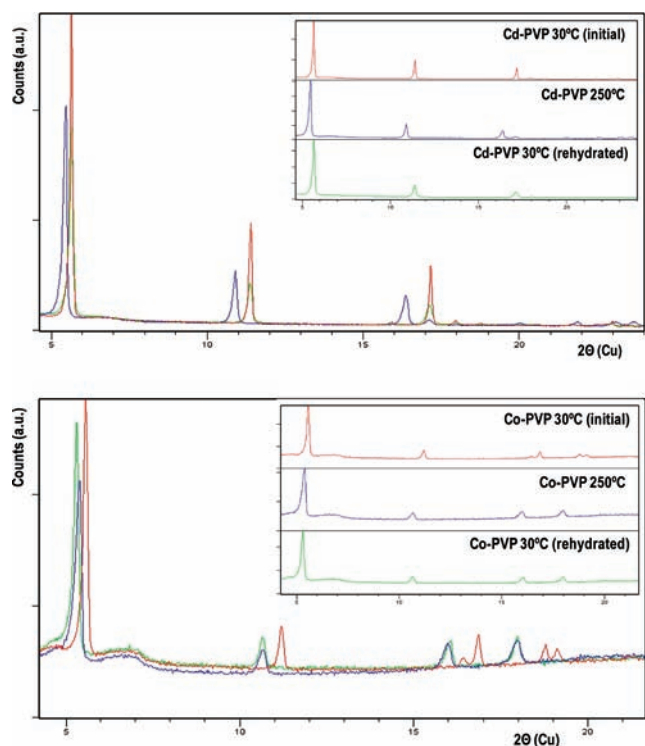**Figure 6.** Thermogravimetric curves for various **M-VP** and **M-PVP** materials.

Figure 7. Dehydration and rehydration of **Cd-PVP** and **Co-PVP**. The individual patterns are more clearly seen in the insets.

Figure 8. Dehydration and rehydration of **Co-VP**.

indicate that the absorption maximum is somewhat lower in wavelength than the 266 nm laser light used to excite the samples. This is the lowest wavelength laser available in the laboratory, and while it is not optimal for exciting the $\pi-\pi^*$ transition in the vinyl group (these excitations are usually around $180-200$ nm) there is sufficient absorption to elicit a response using the intense laser light source. It should be noted that excitation with a hand-held lamp of wavelength 265 nm, typically found in a laboratory, is of insufficient intensity to obtain a visible PL response. The Ni and Co containing materials show peaks in the visible region associated with octahedral co-ordination environments of M^{2+} ions.

The PL emission spectra of the metal vinyl phosphonates (M = Cd, Co, Ni, and Co) show very similar characteristics, with the Zn based material showing a somewhat different response,
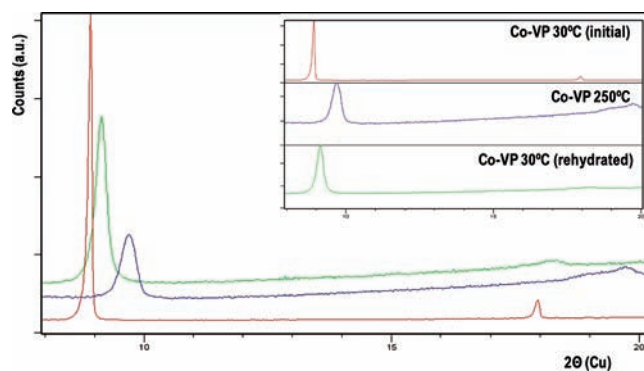
Figure 10. The spectra of the all the vinylphosphonate samples are strikingly similar with peaks being observed around 385 nm, 410 nm, 500 and 510 nm. The higher wavelength signals correspond to green light. The response is not visible to the naked eye as it is very weak, and there is a significant amount of radiation of wavelength 532 nm present because of the harmonic of the laser source. The Zn sample has a relatively strong emission band centered at 383 nm which is due to a $3d^9 4p^1 \rightarrow 3d^{10}$ transition. Given the very different natures of the metals concerned, this leads to the conclusion that the remaining emission peaks arise from a response from the vinyl groups present in the phosphonate anion. It is possible that these are Stokes shifted Raman bands, though at this point it is unclear what the nature of that response might be and further investigation is required using a variable wavelength laser source which would confirm this hypothesis by showing that the position of these bands move as the wavelength of the laser is changed.

The samples based on phenylvinylphosphonic acid all show a strong absorbance around 260 nm, which will is associated with the conjugated phenyl group in the phosphonate anion. Excitation at 266 nm is more efficient for these samples, but once again the PL emissions recorded from the samples are very weak, and require the laser to afford excitation. The PL emission spectra of phenylvinylphosphonic acid and the Cd and Co derivatives present a weak emission at 500 nm. The acid displays a weak band at 610 nm and the Cd derivative a relatively intense peak centered at 621 nm, while no features are observed in this region for the Co derivative.

The weak emission peak at 500 nm is in a location similar to that observed for the vinyl samples, so it would not be unreasonable to ascribe this to the vinyl moiety of the phosphonate anion. The band at 620 nm is a red emission; again it is too weak to be observed by the naked eye. The band at 610 nm is observed for the acid alone, so it must arise from an electronic transition associated with the electronic structure of the organic functional group. It is significantly shifted from the excitation of the phenyl group ($\lambda_{ex} \sim 260$ nm). Again it is possible that these bands have their origins in Raman shifts, but this is only a hypothesis at this point in time. The increase in the emission intensity for the Cd derivative may be explained by considering that the Cd ion is acting as a sensitizer for the Raman emission of the phenyl group in the phosphonate anion. Again a variable wavelength PL study is required to fully elucidate the origins of the observed data.

■ DISCUSSION

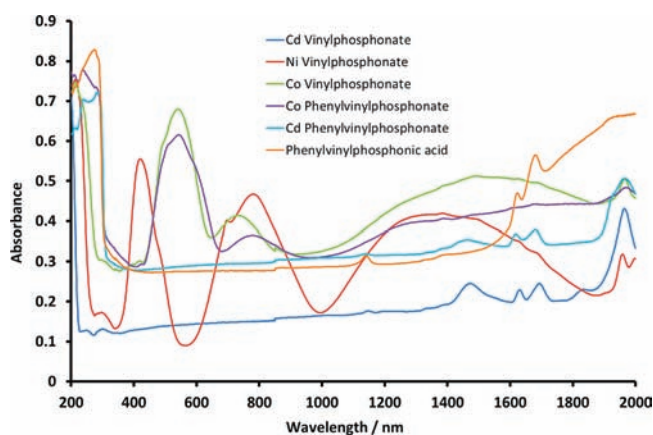As demonstrated, metal vinylphosphonates can have different structures. The same is observed for other phosphonate anions,

Figure 9. Diffuse reflectance UV—vis spectra of **M-VP** and **M-PVP** compounds.
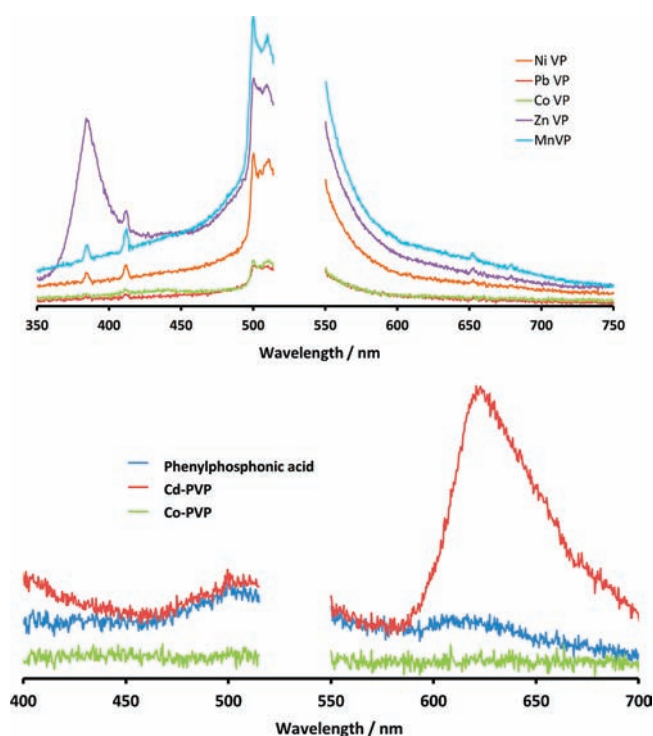

Figure 10. PL emission spectra of **M-VP** (upper) and **M-PVP** (lower) compounds, λ_{ex}= 266 nm. Data are omitted between 525 and 550 nm as they are dominated by a large resonance peak from the 266 nm laser emission.

though this typically occurs where the organic functional group may become involved in coordination to the metal atoms, for example, phosphonocarboxylates.[45a] There are notable exceptions to this observation. The porous structure of β-copper methyl phosphonate is completely different to the structures containing other metals, which are typically layered and crystallize in the $Pmn2_1$ space group. The question to be answered is "what drives the structure to adopt this 3D structure?". Why in a system as reproducible as the vinylphosphonate one, does the anomaly of the Cu material arise? Does it have something to do with copper itself? In the case of the copper methylphosphonate system, this is doubly intriguing since, as well as differing from other methylphosphonates, the nature of the products arising

from the synthesis appear to depend upon the temperature (and hence pressure) of the hydrothermal reaction.

Tetravalent metal phosphonates (e.g., Zn, Ti, Sn), with few exceptions, have layered structures. Comparison of the ionic radii of the tetravalent ions shows very little variation 0.79 Å (Zr), 0.71 Å (Sn), and 0.68 Å (Ti). In divalent metal transition metal ions the radii are broadly similar across the transition series from Mn—Zn with the smallest being low spin Fe^{2+} at 0.61 Å and the largest being Zn at 0.74 Å.

It is noticeable that the radii of the divalent metals are similar to those of the tetravalent metals. It is not therefore surprising that these materials are also layered. The larger radius of the Pb ion on the other hand gives rise to longer bonds and effectively there is more space for coordination around the central atom. This in turn leads to higher coordination numbers, without a significant increase in the O—O distance.

Across the first row of the transition metals, with the exception of Cu, the vinylphosphonates crystallize in the orthorhombic space group $Pmn2_1$. Other metals yield products with the same structure, for example, Cd. Considering the ionic radii with respect to the cell parameters shows some trends, though these are not hard and fast ones. Cd with the largest radius gives the largest cell parameters, whereas Mg with the smallest radius does not yield the smallest values of a, b, and c.

■ CONCLUSION

In this paper a family of **M-VP** (M = Ni, Co, Cd, Mn, Zn, Fe, Cu, Pb; VP = vinylphosphonate) and **M-PVP** (M = Co, Cd; PVP = phenylvinylphosphonate) materials are reported. They have been prepared by hydrothermal syntheses and characterized by FT-IR, elemental analysis, and thermogravimetric methods. Structures were determined either by single crystal X-ray crystallography or from laboratory XRPD data using ab initio methodology. The crystal structure of some **M-VP** and **M-PVP** materials is the "classical" 2D layered, with the organic groups (vinyl or phenylvinyl) extending into the interlamellar space. However, the **Pb-VP** and **Cu-VP** materials show dramatically different structural features. **Pb-VP** has a porous, 3D structure. In that structure the Pb^{2+} center is found in a pentagonal pyramidal environment. Compound **Cu-VP(2)**, a peculiar variant of the common 2D layered structure, possesses a 2D layered structure, but very different from the other **M-VP** materials. It contains three crystallographically distinct Cu centers: an octahedrally coordinated Cu^{2+} ion, a square planar Cu^{2+} ion, and a Cu^+ one. The latter has an unusual co-ordination environment as it is 3-coordinated to two oxygen atoms with the third bond across the double bond of the vinyl group. Metal-coordinated water loss was studied by TGA and thermodiffractometry, which revealed that the rehydration of the anhydrous phases to give the initial phase takes place rapidly for **Cd-PVP** but it takes several days for **Co-PVP**. The **M-VP** materials exhibit variable dehydration—rehydration behavior, with most of them losing crystallinity during the process. The photoluminescence emission spectra of the **M-VP** compounds (M = Cd, Co, Ni, and Co) show very similar characteristics, with the **Zn-VP** showing a somewhat different response. All spectra are strikingly similar and, most likely, the responses arise from the vinyl group.

■ ASSOCIATED CONTENT

ⓢ Supporting Information. CIF files for all structures. XRPD Rietveld plots for compounds **Cd-PVP**, **Cd-VP**, **Co-VP**,

and **Ni-VP**. This material is available free of charge via the Internet at http://pubs.acs.org.

■ AUTHOR INFORMATION

Corresponding Author
*E-mail: gary.hix@ntu.ac.uk (G.B.H.), demadis@chemistry.uoc.gr (K.D.D.), g_aranda@uma.es (M.A.G.A.).

■ ACKNOWLEDGMENT

■ REFERENCES

(1) Jaimez, E.; Hix, G. B.; Slade, R. T. C. *Solid State Ionics* **1997**, *97*, 195.
(2) Giaccomo, P. M. D.; Dines, M. B. *Polyhedron* **1982**, *1*, 61.
(3) Cao, G.; Mallouk, T. E. *Inorg. Chem.* **1991**, *30*, 1434.
(4) Zhang, Y.-P.; Scott, K. J.; Clearfield, A. *Chem. Mater.* **1993**, *5*, 495.
(5) Zhang, Y.-P.; Scott, K. J.; Clearfield, A. *J. Mater. Chem.* **1995**, *5*, 315.
(6) Poojary, D. M.; Clearfield, A. *J. Am. Chem. Soc.* **1995**, *117*, 11278.
(7) Drumel, S.; Janvier, P.; Bujoli-Doeuff, M.; Bujoli, B. *J. Mater. Chem.* **1996**, *6*, 1843.
(8) Bujoli-Doeuff, M.; Evain, M.; Jaffres, P.-A.; Caignaert, V.; Bujoli, B. *Int. J. Inorg. Mater.* **2000**, *2*, 557.
(9) Hartman, S. J.; Todorov, E.; Cruz, C.; Sevov, S. C. *Chem. Commun.* **2000**, 1213.
(10) Gómez-Alcantara, M. M.; Aranda, M. A. G.; Olivera-Pastor, P.; Beran, P.; García-Muñoz, J. L.; Cabeza, A. *Dalton Trans.* **2006**, 577–585.
(11) Yang, C.-Y.; Clearfield, A. *React. Polym.* **1987**, *5*, 13.
(12) Alberti, G.; Casciola, M.; Costantino, U.; Peraio, A.; Montoneri, E. *Solid State Ionics* **1992**, *50*, 315.
(13) Alberti, G.; Casciola, M.; Palombari, R.; Peraio, A. *Solid State Ionics* **1992**, *58*, 339.
(14) Alberti, G.; Casciola, M. *Solid State Ionics* **1997**, *97*, 177.
(15) Liao, T.-B.; Ling, Y.; Chen, Z.-X.; Zhou, Y.-M.; Weng, L.-H. *Chem. Commun.* **2010**, *46*, 1100.
(16) Kirumakki, S.; Huang, J.; Subbiah, A.; Yao, J.; Rowland, A.; Smith, B.; Mukherjee, A.; Samarajeewa, S.; Clearfield, A. *J. Mater. Chem.* **2009**, *19*, 2593.
(17) Wang, Z.; Heising, J. M.; Clearfield, A. *J. Am. Chem. Soc.* **2003**, *125*, 10375.
(18) Clearfield, A. *Prog. Inorg. Chem.* **1998**, *47*, 37.
(19) Jaber, M.; Larlus, O.; Miehe-Brendlé, J. *Solid State Sci.* **2007**, *9*, 144.
(20) Yamazaki, Y.; Jang, M. J.; Taniyama, T. *Sci. Tech. Adv. Mater.* **2004**, *5*, 455.
(21) Taylor, J. M.; Mah, R. K.; Moudrakovski, I. L.; Ratcliffe, C. I.; Vaidhyanathan, R.; Shimizu, G. K. H. *J. Am. Chem. Soc.* **2010**, *132*, 14055.
(22) Chen, Z.; Zhou, Y.; Weng, L.; Yuan, C.; Zhao, D. *Chem.—Asian J.* **2007**, *2*, 1549.
(23) Wharmby, M. T.; Mowat, J. P. S.; Thompson, S. P.; Wright, P. A. *J. Am. Chem. Soc.* **2011**, *133*, 1266.
(24) Yue, Q.; Yang, J.; Li, G.-H.; Li, G.-D.; Chen, J.-S. *Inorg. Chem.* **2006**, *45*, 4431.
(25) Shi, X.; J. Yang, J.; Yang, Q. *Eur. J. Inorg. Chem.* **2006**, 1936.
(26) Colodrero, R. M. P.; Cabeza, A.; Olivera-Pastor, P.; Infantes-Molina, A.; Barouda, E.; Demadis, K. D.; Aranda, M. A. G. *Chem.—Eur. J.* **2009**, *15*, 6612.

(27) Zhang, X.-J.; Ma, T.-Y.; Yuan, Z.-Y. *J. Mater. Chem.* **2008**, *18*, 2003.
(28) Rueff, J.-M.; Barrier, N.; Boudin, S.; Dorcet, V.; Caignaert, V.; Boullay, P.; Hix, G. B.; Jaffrès, P.-A. *Dalton Trans.* **2009**, 10614.
(29) Clearfield, A. *Dalton Trans.* **2008**, 6089.
(30) *APEX2*, V2010.9-1; Bruker AXS Inc.: Madison, WI, 2005.
(31) Sheldrick, G. M. *SADABS, Program for Empirical Absorption Correction of Area Detector Data*; University of Göttingen: Göttingen, Germany, 1997.
(32) Sheldrick, G. M. *Acta Crystallogr.* **1990**, *A46*, 467.
(33) Sheldrick, G. M. *SHELXL-97, Program for the Refinement of Crystal Structures*; University of Göttingen: Göttingen, Germany, 1997.
(34) Boultif, A.; Louer, D. *J. Appl. Crystallogr.* **2004**, *37*, 724.
(35) Cabeza, A.; Losilla, E. R.; Martínez-Tapia, H. S.; Bruque, S.; Aranda, M. A. G. *Adv. X-ray Anal.* **2000**, *42*, 228.
(36) Altomare, A.; Caliandro, R.; Camalli, M.; Cuocci, C.; Giacovazzo, C.; Moliterni, A.; Rizzi, R. *J. Appl. Crystallogr.* **2004**, *37*, 1025.
(37) Rietveld, H. M. *J. Appl. Crystallogr.* **1969**, *2*, 65.
(38) (a) Toby, B. H. *J. Appl. Crystallogr.* **2001**, *34*, 210. (b) Larson, A. C.; von Dreele, R. B. Los Alamos National Laboratory, Report No. LA-UR-86-748, 2000.
(39) Menaa, B.; Kariuki, B. M.; Shannon, I. J. *New J. Chem.* **2002**, *26*, 906.
(40) (a) Knight, D. A.; Kim, V.; Butcher, R. J.; Harper, B. A.; Schull, T. L. *J. Chem. Soc., Dalton Trans.* **2002**, 824. (b) Congiardo, L. K. B.; Mague, J. T.; Funk, A. R.; Yngard, R.; Knight, D. A. *Acta Crystallogr.* **2011**, *E67*, m450.
(41) (a) Zhang, Y.; Clearfield, A. *Inorg. Chem.* **1992**, *31*, 2821. (b) Lebideau, J.; Bujoli, B.; Jouanneaux, A.; Payen, C.; Palvadeau, P.; Rouxel, J. *Inorg. Chem.* **1993**, *32*, 4617.
(42) Hix, G. B.; Turner, A.; Vahter, L.; Kariuki, B. M. *Microporous Mesoporous Mater.* **2007**, *99*, 62.
(43) Barthelet, K.; Nogues, M.; Riou, D.; Férey, G. *Chem. Mater.* **2002**, *14*, 4910.
(44) Drummel, S.; Janvier, P.; Bujoli-Doeuff, M.; Bujoli, B. *Inorg. Chem.* **1996**, *35*, 5786.
(45) (a) Lodhia, S.; Turner, A.; Papadaki, M.; Demadis, K. D.; Hix, G. B. *Cryst. Growth Des.* **2009**, *9*, 1811. (b) Demadis, K. D.; Papadaki, M.; Aranda, M. A. G.; Cabeza, A.; Olivera-Pastor, P.; Sanakis, Y. *Cryst. Growth Des.* **2010**, *10*, 357. (c) Demadis, K. D.; Barouda, E.; Raptis, R. G.; Zhao, H. *Inorg. Chem.* **2009**, *48*, 819. (d) Fernando, I. R.; Daskalakis, N.; Demadis, K.D.; Mezei, G. *New J. Chem.* **2010**, *34*, 221.
(46) Dużak, T.; Zarychta, B.; Olijnyk, V. V. *Inorg. Chim. Acta* **2011**, *365*, 235.
(47) Harrison, W. T. A.; Vaughey, J. T.; Dussack, L. L.; Jacobson, A. J.; Martin, T. E.; Stucky, G. D. *J. Solid State Chem.* **1995**, *114*, 151.

11211

dx.doi.org/10.1021/ic201760w |*Inorg. Chem.* 2011, 50, 11202–11211